Theoretical Modeling of Iron-droplet Combustion Informed by Molecular Dynamics Simulations

L.C. Thijs[a], E. Kritikos[b], A. Giusti[b], W.J.S. Ramaekers[a], J.A. van Oijen[a],
L.P.H. de Goey[a], and X.C. Mi*[a,c]

[a]Department of Mechanical Engineering, Eindhoven University of Technology, Eindhoven, the Netherlands.
[b]Department of Mechanical Engineering, Imperial College, London, United Kingdom.
[c]Eindhoven Institute of Renewable Energy Systems, Eindhoven University of Technology, Eindhoven, the Netherlands.

1 Introduction

Owing to its high energy density, zero-carbon nature, and recyclability, iron powder is nowadays considered as the most promising energy carrier to realize a *Metal-enabled Cycle of Renewable Energy (MeCRE)* on a global scale. [1] To develop real-world combustion systems to harness energy from iron fuel, a key information that the technology developers need to acquire is the heat release rate (HRR) of burning iron particles under various oxidizing gaseous conditions. To obtain this information, an in-depth, quantitative understanding into the fundamentals underlying liquid iron oxidation at elevated temperatures is required. To this end, a research campaign, combining experimental and theoretical efforts, is currently carried out by researchers around the globe.

Although one may argue that studying the laminar flame behaviors can reveal the nature of iron-powder combustion under more application-relevant conditions [2], yet, very little knowledge has been gained via the laminar-flame experiments, which are hindered by an limited amount of data with large uncertainties. Several experimental studies focused on the combustion of isolated iron particles [6, 7], however, have so far provided more useful information to deepen our understanding. Ning et al. [6] first obtain the time-resolved temperature measurement of laser-ignited iron particles burning in gaseous mixtures with various oxygen concentrations (from air to 51% O_2) at room temperature. Panahi *et al.* [7] used a drop-tube furnace to burn iron particles at a high gas temperature (≈ 1350 K) with oxygen concentrations of 21%, 50% and 100%. The time histories of particle temperature obtained from these studies serve as anchor points for us to developing quantitative paradigms to describe the complete combustion process of liquid iron droplets.

In the past few years, the number of theoretical models for single iron particles has increased. A more detailed review of these models can be found in the full preprint of this study [5]. In most of the previously discussed models, the continuum assumption is used to describe the transport processes. It is known that, when the size of the particle becomes too small, modeling the heat and mass transfer using the continuum approach becomes invalid. The particle radius, r_{p}, compared to the mean free path length of the gas molecules, λ_{MFP}, is described by the Knudsen number $\mathrm{Kn} = \lambda_{\mathrm{MFP}}/r_{\mathrm{p}}$. Typically, when Kn is larger than 0.01, the continuum approach is invalid. The effect of heat and mass transfer in

the transition regime (between continuum and free-molecular regimes) on the ignition characteristics of solid iron particles were previously studied. [8] The key finding is that, for iron particles larger $30\,\mu$m, the ignition temperature is less than 3% lower than the prediction of a continuum model. This difference is due the thermal insulating effect in the transition regime. Once a particle ignited, the temperature increases so that λ_{MFP} in the gas-phase boundary layer increase, resulting in a greater value Kn and thus more pronounced effect of transition-regime heat and mass transfer. Thus, this effect must be taken into consideration for modeling the combustion process of a molten iron droplet.

In this abstract, we present the state-of-the-art theoretical model to describe the combustion of a molten iron droplet in a gaseous medium with various O_2 concentrations. Molecular dynamics (MD) simulations are performed to investigate the thermal and mass accommodation coefficients (TAC and MAC, respectively) for the combination of iron(-oxide) and air. TAC described the average energy transfer when gas molecules scatter from the surface. MAC or absorption coefficient quantified the fraction of incoming gas-phase molecules that are absorbed (accommodated) rather than reflected when they collide with the iron surface. The MD-simulation-informed TAC and MAC are incorporated into a zero-dimensional model for the combustion of a single iron particle based on a two-layer configuration to account for the transition-regime heat and mass transfer. The results of particle temperature as a function of time are compared with the recent experimental data. Insights into oxidation mechanism of molten iron droplets are discussed in this abstract.

2 Model description

2.1 Model for single iron particle combustion

The single-particle combustion model is based on the previous work of Thijs *et al.* [4] The detailed formulation of the heat and mass balance equations can be found in [5]. In the liquid phase of an Fe-O mixture, there are no clear crystalline structures, and the molar fraction of O continuously increases in the mixture as more O_2 is absorbed from the surrounding gas. Therefore, the oxidation stage of an iron particle can be characterized by the molar ratio of oxygen, Z_O, defined as

$$Z_O = \frac{m_{O,p}/M_O}{m_{Fe,p}/M_{Fe} + m_{O,p}M_{Fe}},\tag{1}$$

where $m_{O,p}$ is the mass of oxygen, $m_{Fe,p}$ the total mass of iron in the particle, and M_O and M_{Fe} are the molar mass of oxygen and iron, respectively. The thermodynamic properties of an Fe-O mixture at Z_O can be calculated by interpolating the properties of liquid iron, FeO ($Z_O = 0.5$), and Fe_3O_4 ($Z_O = 0.57$), provided in the NASA database.

The two-layer model (shown in Fig. 1(a)) is used approximate the heat and mass transfer in the Knudsen transition regime. The iron particle is surrounded by a spherical Knudsen layer δ with a thickness equal to the mean free path λ_{MFP} of the gas molecules [9]

$$\lambda_{\mathrm{MFP}} = \frac{k_\delta}{p}\frac{\gamma_\delta - 1}{9\gamma_\delta - 5}\sqrt{\frac{8\pi m_{O_2}T_\delta}{k_b}},\tag{2}$$

with k_δ and γ_δ being the thermal conductivity and specific heat ratio derived at the Knudsen layer, p the ambient pressure, m_{O_2} the mass of an oxygen molecule, and k_b the Boltzmann constant. Inside the Knudsen layer, the heat and mass transfer are assumed to be in a free-molecular regime; outside the Knudsen layer, the transport rates are governed by the continuum model. The heat and mass transfer
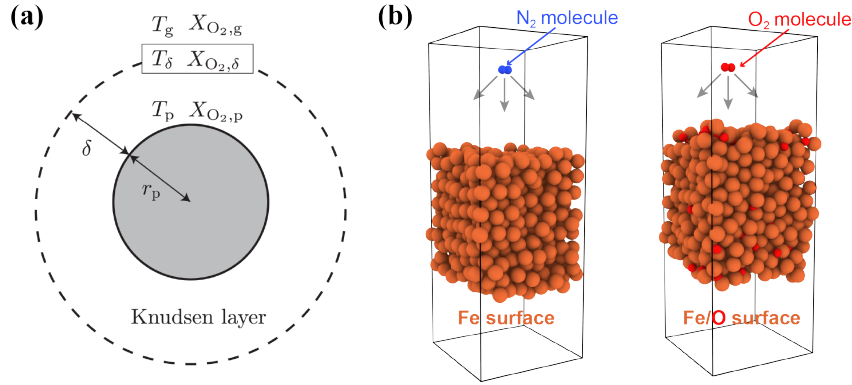
Figure 1: The configuration of (a) the two-layer model for describing the heat and mass transfer in the Knudsen transition regime between a particle and the surrounding and (b) molecular beam simulations for (left) an incident N_2 molecule moving towards an iron surface and (right) an O_2 molecule towards an Fe-O surface.

rates must be equal at the outer surface of the Knudsen layer, i.e., $r = \delta$. The free-molecular-regime O_2 mass and heat transfer rates, $\dot{m}_{O_2,\text{FM}}$ and q_{FM}, can be described as [8]

$$\dot{m}_{O_2,\text{FM}} = \alpha_{\text{m}} \pi r_p^2 v_\delta \rho_{O2,\delta} X_{O_2,\delta}, \tag{3}$$

$$q_{\text{FM}} = \alpha_{\text{T}} \pi r_{\text{p}}^2 p \sqrt{\frac{k_b T_\delta}{8\pi m_{O_2}}} \frac{\gamma^* + 1}{\gamma^* - 1} \left(\frac{T_{\text{p}}}{T_\delta} - 1 \right), \tag{4}$$

where α_{m} and α_{T} are the mass and thermal accommodation coefficients. Since accurate values of TAC and MAC for a surface of liquid Fe-O mixture exposed to O_2 and N_2 gases are unavailable in literature, MD simulations are thus performed to determine their values.

2.2   Model for molecular dynamics simulations

Molecular beam simulations, where a large number of independent scattering events between a single gas molecule and a surface are simulated, are performed [?] to determine the TAC and MAC. For the interaction of N_2 with an iron surface, no chemical absorption is expected. Furthermore, to the authors' knowledge, there is no reactive force field available in the literature for an Fe-O-N system. Therefore, only a TAC value for the nitrogen molecule in combination with an iron surface is determined. As a result, the Fe-N_2 interactions are modeled using non-reactive potentials. On the contrary, reactive molecular dynamics are considered for the Fe_xO_y-O_2 interactions, to compute the TAC and MAC. Large-scale Atomic/Molecular Massively Parallel Simulator (LAMMPS) is used to perform the molecular dynamics simulations. Initial configurations of molecular beam simulations are shown in Fig. 1(b). Detailed description of the MD simulations performed in this study can be found in the preprint [5].

3   Results and discussion

3.1   TAC and MAC obtained from the MD simulations

The TAC for the Fe - N_2 interaction is investigated for a smooth and rough surface. An initially rough surface was created by projecting iron atoms on the initial smooth lattice. Figure 2 (left) shows the TAC of the Fe-N_2 interaction as a function of iron surface temperature for the two different surfaces.

For the smooth surface, the TAC increases as a function of surface temperature from $\alpha_T = 0.08$ up to $\alpha_T = 0.19$. The increasing TAC value can be attributed to the change of a relatively smooth surface in the solid phase into a rough surface in the liquid face when temperature increases. With a rough surface, the TAC values in the solid phase increase to $\alpha_T = 0.17$, almost independent of surface temperature. From the point where the iron surface becomes a liquid (1800 K), the difference between initially smooth and rough surfaces disappears.

The oxygen molecules that do not stick to the surface during Fe_xO_y-O_2 interactions still contribute to the TAC. Figure 2 (right) shows the TAC of the Fe_xO_y-O_2 interaction as a function of Z_O at three different surface temperatures. When the oxidation degree of the surface is low, the TAC remains close to unity but decreases sharply to 0.2 once $Z_O > 0.5$. When iron is burned in air, both oxygen and nitrogen may contribute to the total TAC. Using the results shown in Fig. 2, the total TAC is calculated as

$$\alpha_{T,tot} = [1 - X_{O_2}(1 - \alpha_m)]\alpha_{T,N_2} + X_{O_2}(1 - \alpha_m)\alpha_{T,O_2}. \tag{5}$$
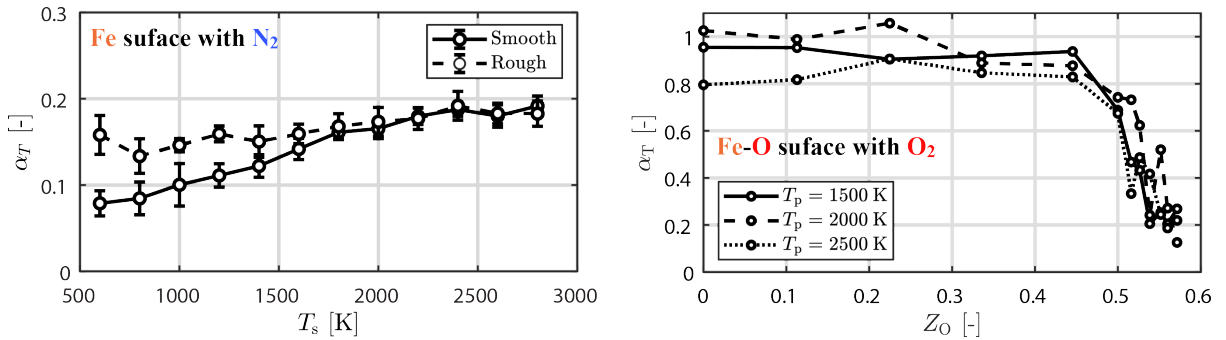
Figure 2: MD-simulation results of TAC (left) as a function of iron surface temperature T_s for N_2 and (right) as a function oxygen molar ratio Z_O of a Fe-O mixture at various surface temperatures.

Figure 3 shows the MAC of oxygen as a function of initial oxidation stage for the three different surface temperatures. The MAC barely depends on the surface temperature and decreases almost linearly as a function of Z_O. Two different slopes are observed, one steeper if $Z_O < 0.5$ and one shallower if $Z_O > 0.5$. When $Z_O > 0.5$, the MAC decreases with a different slope, indicating that once the particle reaches the stoichiometry of FeO, it becomes more difficult to absorb oxygen.
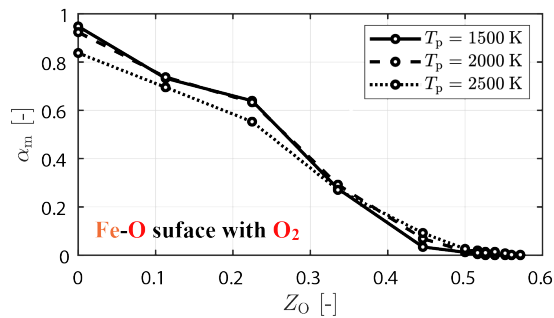
Figure 3: MD-simulation results of MAC as a function oxygen molar ratio Z_O of a Fe-O mixture at various surface temperatures.

3.2   Combustion history of a single iron particle

The results of the MD-informed single-particle combustion model are compared with two sets of experimental data. First, the model is compared to the laser-ignited experiments of Ning *et al.* [6] wherein the particles burn in air at $300\,\mathrm{K}$ as shown in Fig. 4(a). Then, the new temperature curve is compared to the drop-tube experiments of Panahi *et al.* [7] wherein the particles burn in varying oxygen concentrations at $1350\,\mathrm{K}$ as shown in Fig. 4(b)-(d). The experimental data are averaged over multiple independent single-particle measurements to obtain a smooth curve.
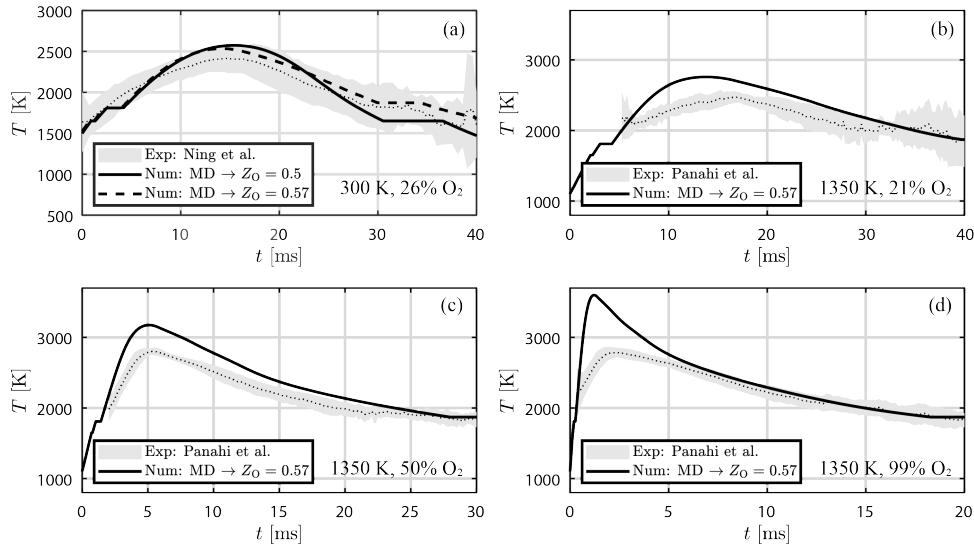
Figure 4: Single-particle model results of iron particle temperature (with an initial particle size of $50\,\mu\mathrm{m}$) as a function of time compared with the experimental data at various ambient gas conditions: (a) a gas temperature of $300\,\mathrm{K}$ with 26% O_2 and (b)-(d) a gas temperature of $1350\,\mathrm{K}$ with 21%, 59%, and 99% O_2, respectively.

Figure 4(a) shows the temperature profiles for the MD-informed Knudsen model with and without further oxidation beyond $Z_O = 0.5$ for a $34\,\mu\mathrm{m}$ and $50\,\mu\mathrm{m}$ particle burning in air with $X_{O_2} = 0.26$. The dotted line and gray area in Fig. 4 are the mean and standard deviation of the experimentally obtained temperature profiles, respectively. The particle temperature for smaller particles is overestimated is overestimated. Overall, the temperature curve obtained with the MD-informed Knudsen model shows a better agreement with the experimentally obtained temperature curve than the continuum-model prediction obtained previously in [4]. Instead of inert cooling after $Z_O = 0.5$, a reactive cooling regime is observed. The new numerically obtained slopes after the peak temperature qualitatively better agree with the experimental measurement during the cooling stage.

Figure 4(b)-(d) shows the temperature profiles for the MD-informed Knudsen model with further oxidation beyond $Z_O = 0.5$ with $X_{O_2} = 0.21$, 0.5 and 0.99 at a gas temperature of $1350\,\mathrm{K}$. Although the model overestimates the particle temperature at the two higher oxygen concentrations, the agreement after the maximum temperature is reasonable. This qualitative agreement implies that the particle keeps on oxidizing after the maximum particle temperature is reached. A possible explanation for the overestimation of the particle temperature at higher oxygen concentrations could be due to the assumption of an infinitely fast internal transport for these high oxygen concentrations. Since for high oxygen concentrations in the gas, the external diffusion of oxygen is fast, the diffusion of oxygen in the condensed phase could be rate-limiting. A new model incorporating the mechanism of internal transport is under development and will be presented at the Colloquium.

4   Summary of key findings

Molecular dynamics simulations have been performed to investigate the thermal and mass accommodation coefficients for the combination of iron(-oxide) and air. By incorporating the MD information into the single iron particle model, a new temperature-time curve for the single iron particles is observed compared to results obtained with previously developed continuum models. Since the rate of oxidation slows down as the MAC decreases with an increasing oxidation stage, the rate of heat release decreases when reaching the maximum temperature, such that the rate of heat loss exceeds that of heat release. In addition, the oxidation beyond $Z_O = 0.5$ (from stoichiometric FeO to Fe_3O_4) is modeled. The effect of the transition-regime heat and mass transfer on the burn time becomes more than 10% if the particles are smaller than 10 μm. In the cases with sufficiently high O_2 concentrations in the ambient gas, the model overestimates the particle temperature, indicating that the rate of internal transport could become important, and therefore limit the maximum temperature.

References

[1] Bergthorson, J. M. (2018). Recyclable metal fuels for clean and compact zero-carbon power. Prog. Energy Combust. Sci. 68: 169-196.

[2] Goroshin, S., Palecka, J., Bergthorson, J. M. (2022). Some fundamental aspects of laminar flames in nonvolatile solid fuel suspensions. Prog. Energy Combust. Sci. 91: 100994.

[3] Mi, X., Fujinawa, A., & Bergthorson, J. M. (2022). A quantitative analysis of the ignition characteristics of fine iron particles. Combustion and Flame, 240: 112011.

[4] Thijs, L. C., van Gool, C. G., Ramaekers, W. J. S., Kuerten, J. G. M., van Oijen, J. A., & de Goey, L. P. H. (2022). Improvement of heat-and mass transfer modeling for single iron particles combustion using resolved simulations. Combustion Science and Technology, 1-17.

[5] Thijs, L. C., Kritikos, E., Giusti, A., Ramaekers, W. J., van Oijen, J. A., de Goey, L. P., & Mi, X. C. (2022). On the combustion of fine iron particles beyond FeO stoichiometry: Insights gained from molecular dynamics simulations. arXiv preprint arXiv:2212.06432.

[6] Ning, D., Shoshin, Y., van Stiphout, M., van Oijen, J., Finotello, G., de Goey, P. (2022). Temperature and phase transitions of laser-ignited single iron particle. Combustion and Flame, 236, 111801.

[7] Panahi, A., Chang, D., Schiemann, M., Fujinawa, A., Mi, X., Bergthorson, J. M., Levendis, Y. A. (2023). Combustion behavior of single iron particles-part I: An experimental study in a drop-tube furnace under high heating rates and high temperatures. Applications in Energy and Combustion Science, 13, 100097.

[8] Jean-Philyppe, J., Fujinawa, A., Bergthorson, J., Mi, X., 2022. The ignition of fine iron particles in the knudsen transition regime, preprint on ResearchGate.

[9] Liu, F., Daun, K.J., Snelling, D.R., Smallwood, G.J. (2006). Heat conduction from a spherical nano-particle: status of modeling heat conduction in laser-induced incandescence. Applied physics B, 83, 355-382.

[10] Sipkens, T.A., Daun, K.J. (2018). Effect of surface interatomic potential on thermal accommodation coefficients derived from molecular dynamics. The Journal of Physical Chemistry C, 122(35), 20431-20443.